Volume 22
Number 16
28 April 2020
Pages 8239–9158

PCCP

Physical Chemistry Chemical Physics

rsc.li/pccp

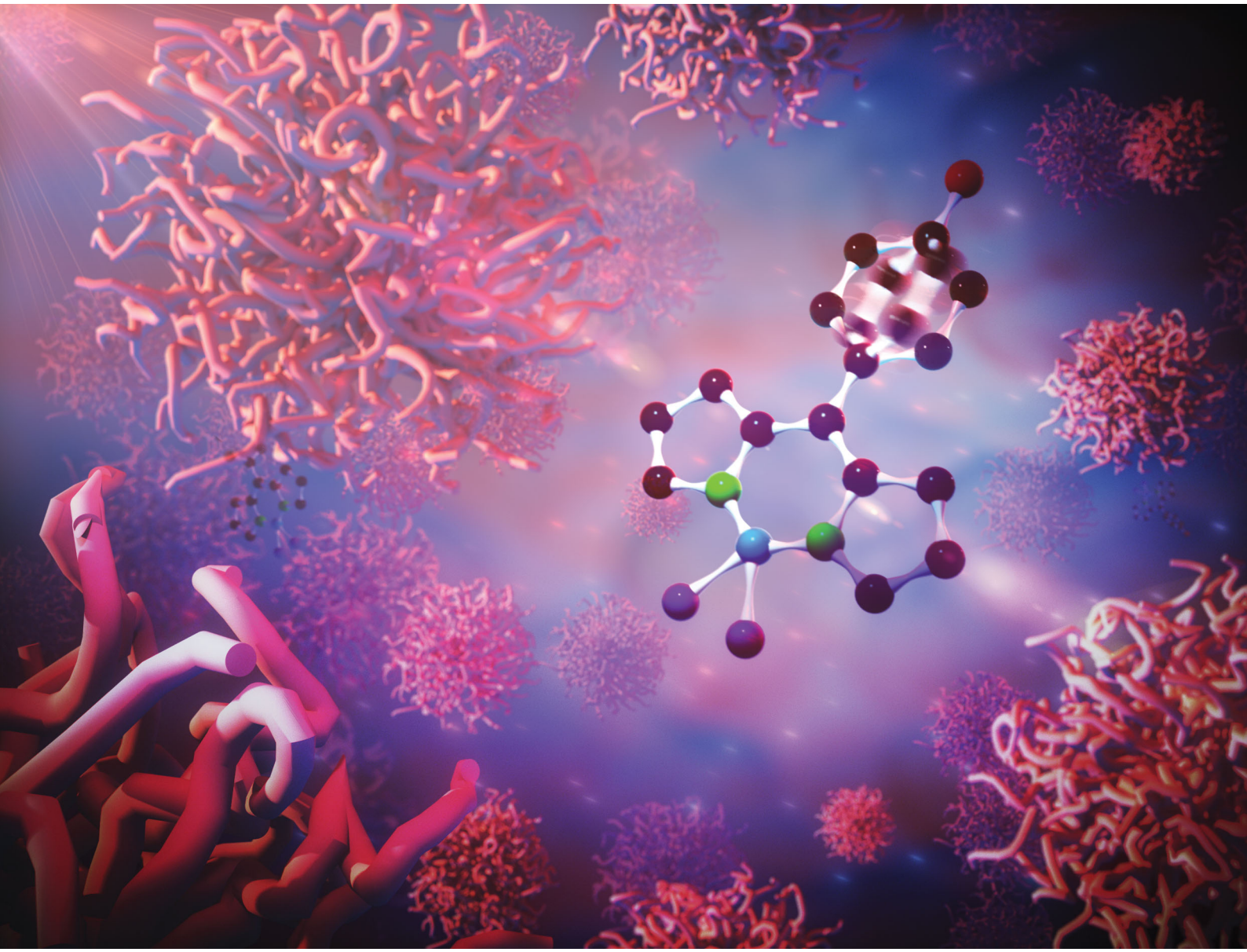

ISSN 1463-9076

ROYAL SOCIETY OF CHEMISTRY

PAPER

Aurimas Vyšniauskas *et al.*

The effect of solvent polarity and macromolecular crowding on the viscosity sensitivity of a molecular rotor BODIPY-C_{10}

PCCP

PAPER

View Article Online
View Journal | View Issue

Check for updates

Cite this: *Phys. Chem. Chem. Phys.*, 2020, **22**, 8296

The effect of solvent polarity and macromolecular crowding on the viscosity sensitivity of a molecular rotor BODIPY-C_{10}†

Artūras Polita,‡[a] Stepas Toliautas,[b] Rokas Žvirblis[a] and Aurimas Vyšniauskas *[a]

Received 20th December 2019,
Accepted 19th February 2020

DOI: 10.1039/c9cp06865a

rsc.li/pccp

Viscosity is the key parameter of many biological systems as it influences passive diffusion, affects the lipid raft formation and plays a significant role in several diseases on a cellular level. Consequently, determination of precise viscosity values is of great interest and viscosity-sensitive fluorescent probes offer a convenient solution for this task. One of the most frequently used viscosity-sensitive probes is BODIPY-C_{10}. Yet despite its regular use, BODIPY-C_{10} remains insufficiently investigated. In this work, we explored how the polarity, hydrogen bonding abilities of the solvent and the presence of macromolecules affect the viscosity-sensing qualities of BODIPY-C_{10}. In addition, we investigated the relaxation pathway of BODIPY-C_{10} with the help of femtosecond transient absorption and time-dependent DFT calculations. Our results show that while BODIPY-C_{10} is not affected by protic solvents, accurate quantitative determination of viscosity is possible only if BODIPY-C_{10} is calibrated in the same polarity environment as in the sample of interest, and the size of the surrounding molecules is not larger than the size of BODIPY-C_{10}. The latter limitation is likely to apply to all molecular rotors.

Published on 20 February 2020. Downloaded on 4/30/2020 5:26:52 AM.

Introduction

One of the basic physical properties of a cell is viscosity – it determines diffusion coefficients of macromolecules and controls the passive transport of molecules across the plasma membrane. Precise determination of viscosity values within the cell would benefit the current understanding of membrane dynamics, lipid raft formation and even assist in unveiling molecular biology of Alzheimer's disease[1] or diabetes.[2]

Due to the small scale of cellular objects, it is inherently difficult to perform accurate mechanical viscosity measurements in such systems. Furthermore, biological objects are highly inhomogeneous and viscosity values of the plasma membrane, or cytoplasm, will differ across the measured object. However, precise and quantitative viscosity measurements on a small scale can easily be made using a fluorescent class of compounds termed molecular rotors.[3–5] Moreover, molecular rotors are able to produce spatial viscosity maps when paired with fluorescence lifetime imaging microscopy (FLIM).[6–8]

In the excited state, molecular rotors undergo conformational changes, which result in a molecular rotor leaving the fluorescent state.[3] As conformational motion rate is directly influenced by viscosity, molecular rotors display great fluorescence lifetime and fluorescence intensity sensitivity to local viscosity values.[9] Higher local viscosity impedes conformational changes of the molecular rotor, and the fluorescence intensity and fluorescence lifetime increases.[9] As fluorescence intensity is dependent on the local concentration of a fluorophore, it is convenient to evaluate viscosity values from fluorescence lifetime, which is independent of the fluorophore concentration.

Currently, one of the most extensively used molecular rotors is BODIPY-C_{10} and its longer variant with equivalent photophysical properties BODIPY-C_{12} (Fig. 1), both molecules referred to as BODIPY-C_n later in the text. One of the main advantages of BODIPY-C_n is monoexponential fluorescence decay compared to molecular rotors possessing multiexponential fluorescence decay kinetics.[10] Since only a few hundred photons are required for reliable monoexponential fluorescence decay fitting,[11] a smaller fluorescence signal and quicker acquisition time are sufficient when performing FLIM measurements. Previously, BODIPY-C_n and its derivatives have been used for viscosity sensing in aerosols,[12] polymers,[13] lipid microbubbles,[14] model lipid membranes,[15–18] membranes of an eye lens,[19] malignant tissues,[20] live cells[6] and its organelles: plasma membrane,[21–23] endoplasmic reticulum,[24] nucleus,[25]

[a] *Center of Physical Sciences and Technology, Saulėtekio av. 3, Vilnius, LT-10257, Lithuania. E-mail: aurimas.vysniauskas@ftmc.lt*
[b] *Institute of Chemical Physics, Faculty of Physics, Vilnius University, Saulėtekio av. 9-III, 10222 Vilnius, Lithuania*

† Electronic supplementary information (ESI) available. See DOI: 10.1039/c9cp06865a

‡ Current address: Department of Chemistry, Aarhus University, Langelandsgade 140, Aarhus C, 8000, Denmark.

This journal is © the Owner Societies 2020

Published on 20 February 2020. Downloaded on 4/30/2020 5:26:52 AM.

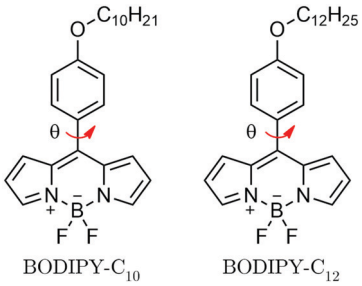

Fig. 1 Structures of two variants of one of the most widely used molecular rotor BODIPY-C_n. Red arrow indicates intramolecular rotation which causes BODIPY-C_n to display viscosity sensitivity.

mitochondrium[26] or multiple organelles using protein-tag techniques.[27,28]

Surprisingly, despite its broad applicability, photophysical properties of BODIPY-C_n remain insufficiently investigated. For instance, it was discovered that the fluorescence lifetime of BODIPY-C_n is not exclusively dependent on viscosity, but is also influenced by other physical properties of the solvent.[29] Even though BODIPY-C_n displays insignificant solvatochromic shift,[10] its fluorescence lifetime was shown to be greater in toluene by the factor of 2 compared to methanol.[29] It remains unclear whether this difference is an outlier or a part of a general trend. Such difference suggests that BODIPY-C_n is influenced by the polarity of the solution or perhaps that BODIPY-C_n participates in hydrogen bonding with the surrounding molecules. Inside the cells, there are vastly different environments ranging from polar-protic cytoplasm to the hydrophobic-aprotic interior of the plasma membrane. In addition to contrasting polarities and hydrogen bonding capabilities, there are also great differences between the sizes of the molecules inside the cell. Currently, the influence of the molecular size on fluorescence lifetime of BODIPY-C_n – or of any other molecular rotor – has been explored very little with only one existing work[28] known to us. Since molecular rotors sense viscosity on a microscopic level, the size of surrounding molecules might impact their response even if bulk viscosity remains the same. Therefore, a comprehensive understanding of BODIPY-C_n interactions with the surrounding environment is crucial if measured viscosity values in living systems are to be trusted. Finally, it remains unknown what happens to excited BODIPY-C_n when it leaves the fluorescent state. Knowing the nature of "dark" states the molecule passes through on its journey back to the ground state would help to better understand the precise viscosity-sensing mechanism and origins of undesired sensitivity to other properties of the environment besides viscosity.

Here, we investigate how hydrogen bonding and solvent polarity affect the fluorescence lifetime of BODIPY-C_n by empirically plotting the fluorescence lifetimes of BODIPY-C_{10} *versus* viscosity in different types of low viscosity solvents (polar-protic, polar-aprotic, nonpolar-protic, and nonpolar-aprotic) and solvent mixtures of higher viscosity. Furthermore, by performing femtosecond transient absorption experiments, we investigate the molecular relaxation mechanism of BODIPY-C_{10} at varying viscosities and compare the result with theoretical time-dependent density functional theory (TD-DFT) calculations. Finally, by using polymer solutions we explore the influence of large surrounding molecules on the fluorescence lifetime of BODIPY-C_{10} molecular rotors and demonstrate that microviscosity experienced by BODIPY-C_{10} in some instances may be very different to the bulk viscosity of the solution. Our results obtained for BODIPY-C_{10} are very likely to be valid for all BODIPY-C_n molecular rotors bearing an ether group given the insignificant influence the alkyl chain has on the photophysics of the rotor.[29]

Methods and materials

Dyes, reagents, and solvents

BODIPY-C_{10} was synthesised as previously reported.[30] Stock solutions of BODIPY-C_{10} were prepared in methanol and diluted for further experiments in solvents or their mixtures. Castor oil, isopropanol, methanol, ethanol, cyclohexane, dimethylformamide (DMF), dimethyl sulfoxide (DMSO), toluene, chloroform, dichloromethane (DCM), acetone, acetonitrile, tetrahydrofuran (THF), cyclohexanone, 1,2-dichloroethane (EDC), chlorobenzene, diethyl ether, and pentane were obtained from Sigma. Average molar masses of polymethyl methacrylate (PMMA) (Sigma) were 15 kDa and 1 MDa. Average molar masses of polyethylene glycol (PEG) (Sigma) were 20 kDa, 4 kDa, and 0.5 kDa. Polymer solutions and solvent mixtures were made by mixing reagents at different ratios. Calculated orientation polarisation values for low viscosity solvents are listed in Table 1. Viscosities of pure solvents, relative permittivity values and refractive indexes were taken from Lange's Handbook of Chemistry.[31]

Viscosity measurements in polymer solutions

Viscosities of PMMA and PEG polymer solutions and solvent mixtures were measured using vibrational viscometer (SV-10, A&D); viscosities of PMMA solutions and solvent mixtures were measured at 22 °C, whilst viscosities of 20 kDa, 4 kDa and 0.5 kDa PEG solutions were recorded at 30 °C, 22 °C, and 4 °C, respectively.

Table 1 Orientation polarisability (eqn (2)), refractive index and relative permittivity values for pure solvents

Solvent	Δf	n	ε
Pentane	−0.007	1.3575	1.837
Cyclohexane	0.0018	1.4262	2.05
Toluene	0.0136	1.4969	2.385
Chlorobenzene	0.1443	1.5248	5.69
Chloroform	0.1479	1.4467	4.807
Diethyl ether	0.1641	1.3538	4.267
THF	0.2095	1.4052	7.52
DCM	0.2190	1.4237	9.14
EDC	0.2218	1.4443	10.5
Cyclohexanone	0.2427	1.4507	16.1
DMF	0.2751	1.4305	38.25
Isopropanol	0.2766	1.3772	20.18
DMSO	0.2833	1.4170	47.24
Acetone	0.2835	1.3620	21.0
Ethanol	0.2897	1.3610	25.3
Acetonitrile	0.3042	1.3460	36.64
Methanol	0.3091	1.3276	33.0

Published on 20 February 2020. Downloaded on 4/30/2020 5:26:52 AM.

The polymer content (w/w%) in solutions was: 10% to 95% (0.5 kDa PEG in methanol), 20% to 60% (4 kDa PEG in methanol), 10% to 50% (20 kDa PEG in methanol), 1% to 15% (1 MDa PMMA in toluene).

Absorption, steady-state, and time-resolved fluorescence

Absorption spectra were measured using Jasco V-670 spectrophotometer. Fluorescence spectra were recorded with Edinburgh-F900 (Edinburgh Instruments) fluorimeter using 1 MHz frequency picosecond pulsed diode laser EPL-470 (Edinburgh Instruments) emitting at 473 nm as an excitation source. Fluorescence decays were measured using time-correlated single-photon counting. Fluorescence decays had 5000 counts at the peak of the decay with 50 ns window being used with 4096 channels. Both 1 mm and 10 mm quartz cuvettes were used for absorption and fluorescence measurements with BODIPY-C_{10} concentration being up to 20 μM. Fluorescence decays of BODIPY-C_{10} in solvent mixtures, pure solvents, and PMMA solutions were taken at 22 °C, while decays of 20 kDa PEG, 4 kDa PEG and 0.5 kDa PEG solutions were recorded at 30 °C, 22 °C and 4 °C, respectively. Measurements were performed at these temperatures either to reach higher viscosities (0.5 kDa PEG) or to increase the solubility of PEG in methanol (20 kDa PEG).

Femtosecond transient absorption

Pharos 10-600-PP (Light Conversion Ltd) laser producing 290 fs pulses at 1028 nm, 4.76 kHz frequency was used as an excitation source. Orpheus PO15F2L (Light Conversion Ltd) collinear optical parametric amplifier was used for controlling the output laser wavelength. The pumping wavelength was set to 480 nm, whereas the probe beam was sent through a Ti:sapphire crystal for generating 485–700 nm continuum. The difference of polarisation of both beams was set to the magic angle in order to cancel out the changes in signal due to the rotation of the excited fluorophores in solution. Andor-Shamrock SR-500i-R (Andor technology) spectrometer was used together with Andor-Newton DU970 CCD (Andor Technology) camera (1600 × 200 pixels) for detecting the transient absorption signal. The concentration of BODIPY-C_{10} was 40 μM resulting in the optical density of solution equal to 0.3.

Theoretical calculations

Quantum chemical calculations of the molecular properties were performed using electronic structure modelling package Gaussian09[32] at the level of density-functional theory[33] (DFT, for the ground-state properties) and the time-dependent DFT[34] (for the excited-state properties). M06-2X hybrid functional[35] and cc-pVDZ basis set[36] were used for all computations, while averaged solvent effect on the solute was modelled using C-PCM[37] with solvent parameters of toluene and DMF.

Data analysis

Fluorescence decays of BODIPY-C_n were fitted using Edinburgh-F900 software package F900. For pure solvents, PMMA and PEG polymer solutions, monoexponential decay model was applied. For solvent mixtures containing Castor oil, which is fluorescent itself, biexponential fluorescence decay model was applied, and intensity-weighted mean lifetimes (1) were chosen for lifetime–viscosity plots:

$$\tilde{\tau} = \frac{\sum_i a_i \tau_i^2}{\sum_i a_i \tau_i} \quad (1)$$

where a_i and τ_i are the amplitudes of individual components. The goodness-of-fit parameter (χ^2) was 1.5 or less for single decays. Polarities of pure solvents were ranked (Table 1) using Lippert's equation[38] (2) which describes orientation polarisability of the solvent:[38]

$$\Delta f = \frac{\varepsilon - 1}{2\varepsilon + 1} - \frac{n^2 - 1}{2n^2 + 1} \quad (2)$$

where ε is a relative permittivity and n is the refractive index of a pure solvent. Global analysis of transient absorption spectroscopy data was performed using Glotaran 1.5.1.[39]

Results and discussion

Influence of solvent polarity and proticity

In order to investigate the sensitivity of BODIPY-C_{10} to other solvent properties besides viscosity, such as polarity and the capability of forming hydrogen bonds, we did measurements in a number of protic and aprotic solvents of different polarities (Fig. 2).

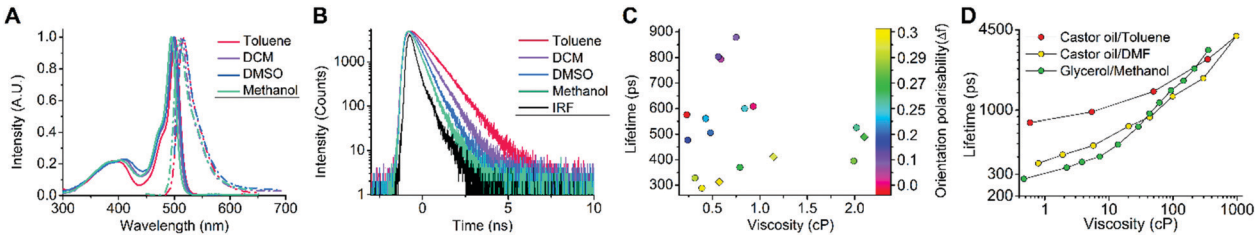

Fig. 2 (A) Fluorescence (dot-dashed lines) and absorption (solid lines) spectra of BODIPY-C_{10} obtained in toluene, DCM, DMSO and methanol. (B) Time-resolved fluorescence decays of BODIPY-C_{10} in toluene, DCM, DMSO, and methanol. (C) Colour-coded fluorescence lifetimes of BODIPY-C_{10} obtained in protic (diamonds) and aprotic (circles) solvents of varying orientation polarisability (polarity). (D) Fluorescence lifetimes of BODIPY-C_{10} obtained in non-polar Castor oil–toluene (red dots), relatively polar Castor oil–DMF (yellow dots) and polar glycerol–methanol (green dots) solvent mixtures of varying viscosity.

 This journal is © the Owner Societies 2020

Published on 20 February 2020. Downloaded on 4/30/2020 5:26:52 AM.

Previously, it has been shown that the Lippert plot for BODIPY-C_{12} has a slope of almost zero,[10] which might suggest that BODIPY-C_n is completely insensitive to solvent polarity. Our absorption and fluorescence spectra of BODIPY-C_{10} confirm this result (Fig. 2A). However, BODIPY molecular rotors are applied as lifetime sensors, *i.e.* the viscosity of their environment is estimated from the numerical value of the fluorescence lifetime of the fluorophore. Therefore, the influence of solvent polarity and its proticity (the ability to form hydrogen bonds) on fluorescence lifetime needs to be assessed as well. Our results show (Fig. 2) that despite the fact that the absorption and emission spectra in solvents of contrasting polarity look almost identical, the time-resolved fluorescence decays of BODIPY-C_{10} in those very same solvents yield significantly different lifetime values (Fig. 2B and C). In order to further investigate the influence of polarity and proticity, we performed time-resolved fluorescence measurements in 17 solvents of different polarities ranging from pentane to methanol, with a handful of them having the capability to form hydrogen bonds, which are shown as diamonds in Fig. 2C. The colour of data points in Fig. 2C denotes orientation polarisability of the solvent (eqn (2)), with low values of orientation polarisability common for non-polar solvents, and *vice versa*. As evident from Fig. 2C, in solvents, the fluorescence lifetimes of BODIPY-C_{10} are largely influenced not by viscosity, but by polarity. For example, in the solvents of $\sim$0.5 cP viscosity, BODIPY-C_{10} possesses fluorescence lifetimes ranging from 300 to 800 ps (Fig. 2C). We have also determined fluorescence quantum yields in those solvents and then used them together with lifetimes to calculate radiative and non-radiative decay constants (Fig. S1, ESI†). The results show that the variation in non-radiative decay constants mostly determines the variation in fluorescence lifetimes. It is important to note that the protic solvents (diamonds in Fig. 2C) do not stand out from their counterparts with similar orientation polarisability. Therefore, while BODIPY-C_{10} is affected by the solvent's polarity, it is not dependent on the solvent's ability to form hydrogen bonds.

BODIPY-C_n is generally used in membranes where viscosity can be higher by two orders in magnitude compared to common organic solvents. In order to assess the susceptibility of BODIPY-C_{10} to solvent's polarity at higher viscosity, we prepared solventmixtures of varying viscosity from DMF (relatively polar, non-viscous) and Castor oil (non-polar, viscous). Then we compared the lifetimes of BODIPY-C_{10} in the aforementioned mixtures to the ones in toluene (non-polar, non-viscous), and Castor oil mixtures. For comparison, we have also added methanol–glycerol (very polar, viscous) solvent mixtures from Vysniauskas *et al.*[29] Fig. 2D shows a clear mismatch between lifetime–viscosity dependences in both solvent mixtures. We found that the lifetime of BODIPY-C_{10} remains susceptible to polarity at high viscosities as well, although not as much as at low viscosities (Fig. 2D). The difference between the lifetimes at about 500 cP is relatively small compared to the difference between the lifetimes at 1 cP (Fig. 2D). Since the most frequent application of molecular rotors is a quantitative determination of viscosity in highly heterogeneous systems such as live cells or their organelles, the fact that the fluorescence decay rates of BODIPY-C_{10} are polarity-dependent means that the rotor needs to be calibrated in solvent mixtures that have closely similar polarity to the inner environment of the organelle of interest. Otherwise, an erroneous viscosity value is likely to be obtained. On the other hand, if one is interested in measuring only a qualitative, but not a quantitative change in viscosity, such calibration is not necessary.

TD-DFT calculations

The fact that solvent polarity heavily influences fluorescence lifetime of BODIPY-C_{10}, but not its steady-state spectra, signifies that the fluorescent state of the rotor is not affected by polarity. The state that is affected is the one the rotor goes to upon leaving the fluorescent state. If it gets stabilised in a high polarity environment, it could be expected that the transition out of the fluorescent state should be faster. To explore this possibility, we have performed a time-dependent density functional theory (TD-DFT) calculations. The potential energy with respect to the dihedral angle Θ between the phenyl ring and the BODIPY core (Fig. 1) is shown in Fig. 3. Solvent effect of toluene was included in the calculations. Furthermore, to reduce calculation times, alkyl substituent was shortened from 10 or 12 carbon atoms to one. We have checked that this has no influence on our results by performing calculations on a molecule with $-OC_4H_9$ group, which resulted in identical energy curves (Fig. S2, ESI†).

The shape of the potential energy curve closely agrees to the ones calculated for similar BODIPY fluorophores that bear other substituents in the place of the ether group in BODIPY-C_n.[40,41] Upon excitation the fluorophore enters the excited state close to the local minimum $S_{1,m}$ (Fig. 3). From there it can either stabilize in $S_{1,m}$ and relax radiatively or surmount a relatively small ($\sim$0.07 eV) potential energy barrier and reach another minimum $S_{1,r}$, from where the molecule should rapidly relax back to the ground state through a nearby conical intersection.[42] The obtained energy barrier is not far off from the one estimated from the temperature dependence of fluorescence lifetime of BODIPY-C_{10} (11 kJ mol^{-1} or 0.11 eV).[29]

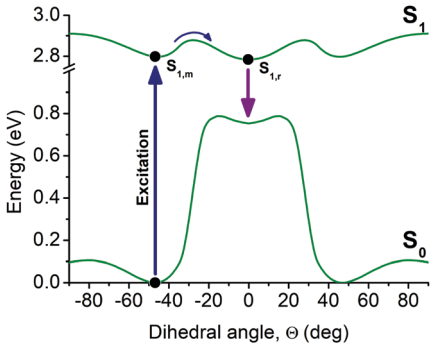

Fig. 3 Potential energy curves of the ground (S_0) and the first excited electronic state (S_1) of BODIPY-C_{10} obtained from TD-DFT calculations. Θ is a dihedral angle between a phenyl ring and a BODIPY core as shown in Fig. 1. The black dot at $\sim$50° denotes the ground state minimum and the position on the potential energy curve the fluorophore takes upon excitation. When the barrier at $\sim$25° is surmounted the fluorophore reaches excited state minimum $S_{1,r}$ from where it rapidly relaxes back to the ground state *via* a nearby conical intersection.

Published on 20 February 2020. Downloaded on 4/30/2020 5:26:52 AM.

We have also performed the same calculations with DMF as a solvent, where the lifetime of BODIPY-C_{10} was 370 ps instead of 793 ps as in toluene. However, the modelling results did not reveal why BODIPY-C_n has a shorter lifetime in polar solvents.

The calculated results in DMF show slightly higher energy barrier as well as the higher energy of $S_{1,r}$ state (Fig. S3, ESI†), which, omitting other factors, should lead to a longer lifetime as a higher barrier would make it more difficult for the fluorophore to reach $S_{1,r}$ geometry and relax to the ground state. In our previous work we have shown that subtle changes in the shape of the potential energy surface can lead to an increase in fluorescence lifetime by a factor of 6.[41] Therefore, the origins of a shorter fluorescence lifetime of BODIPY-C_{10} by a factor of ~1.5–2 in polar solvents could be caused by an additional property not explicitly taken into account during TD-DFT calculations performed here.

Nevertheless, previous theoretical results on BODIPY molecules similar to BODIPY-C_n suggest that an unsaturated substituent in the 5′ position on the BODIPY core facilitates the formation of the partial charge transfer state upon excitation.[42,43] Such state would be more stabilised by polar solvents, which, in the case of BODIPY-C_n, would stabilise $S_{1,r}$ geometry to the greater degree than the others due to the fact that the phenyl ring is in conjugation with the BODIPY core and partial charge transfer is more likely. This would reduce the energy barrier thus reducing the fluorescence lifetime.

Femtosecond transient absorption

In order to extract more information about the relaxation pathway of BODIPY-C_{10}, we have performed transient absorption spectroscopy. As solvents, we chose toluene (non-polar), methanol (polar) and glycerol–methanol mixtures up to 70% of glycerol (v/v%). Solvents were chosen to determine how viscosity and polarity can affect the relaxation pathway of BODIPY-C_{10}. Transient absorption spectra consisted of a single negative band (Fig. 4A), which is a result of overlapping ground state bleach (GSB) (<510 nm) and stimulated emission (SE) (>510 nm) bands. The shapes and positions of bands were similar in all solvents; the only difference is slower decay times in more viscous solvents (Fig. S4, ESI†). The fact that the GSB band is short-lived and decays to 0 in 1000 ps in low viscosity solvents indicates that no triplet states are formed.

Next, a global analysis of transient absorption data was performed. Two components were required to successfully fit the data in all solvents except for 70% glycerol–methanol mixture, where a single component was sufficient. Both exponential components can be clearly seen at 520 nm, where stimulated emission dominates (Fig. 4B), while the ground state bleach band (495 nm) decays with a single lifetime. The full picture is revealed by the decay associated spectra (Fig. 4C), which shows that the short lifetime component is situated only at higher wavelengths where SE band dominates. Therefore, the short-lived component represents a partial relaxation of the molecule in the fluorescent state, resulting in a significant drop in its oscillator strength and, therefore, fast, but not a total reduction in stimulated emission. In contrast, the long-lived component represents a complete relaxation from the fluorescent state as evident from its close similarity to the fluorescence lifetime of BODIPY-C_{10} (Fig. 4D). Since GSB band also decays with this lifetime, it means that the fluorophore returns to the ground state immediately upon leaving the fluorescent state.

Solvent polarity does not affect the short lifetime but this lifetime is affected by viscosity. This means that the initial relaxation is not likely to involve partial charge transfer but a significant change in molecular geometry is possible, similar to the final relaxation from the fluorescent state corresponding to the long lifetime. The most likely assignment of the initial transition is relaxation from the Franck–Condon (FC) state to the local minimum $S_{1,m}$ (Fig. 3). Other options are either too fast (vibrational relaxation) or should not result in the reduction of the oscillator strength (solvent relaxation). The similar assignment was made in the previous work by Suhina *et al.* where a BODIPY rotor with an ester group was examined.[40] The observed drop in oscillator strength upon partial relaxation as evident from the fast decrease in stimulated emission most likely happens due to the out-of-plane distortion of the BODIPY core,[42,44,45] where both HOMO and LUMO are localised at ground state geometry.[45] This is supported by time-resolved infrared spectroscopy results on a similar fluorophore showing that after initial relaxation a band appears at 1520 cm^{-1}, where vibrations of the BODIPY core are expected.[40] We note that the out-of-plane distortion also accompanies the rotation of the phenyl ring during the relaxation of the molecule.[41,42]

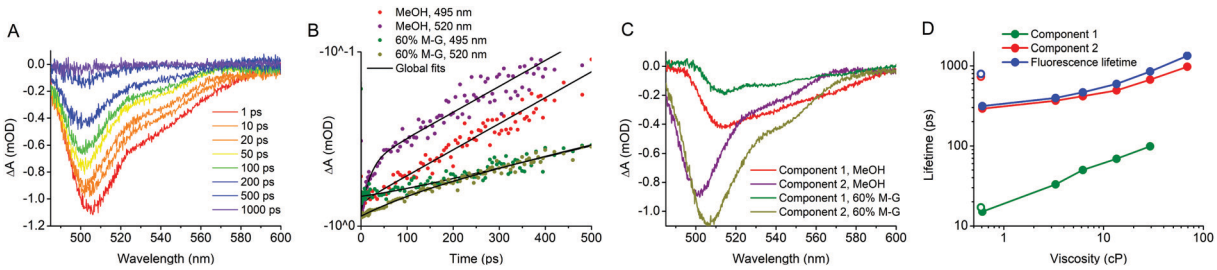

Fig. 4 (A) Transient absorption spectra of BODIPY-C_{10} in methanol at different pump–probe delay times. (B) Transient absorption traces at 495 nm (ground state bleach) and 520 nm (stimulated emission) in methanol and 60% glycerol–methanol mixture. (C) Decay associated spectra of two components obtained from the global analysis of transient absorption data. (D) Lifetimes of individual components shown in (C) in toluene (empty circles) and glycerol–methanol mixtures ranging from 0% to 70% of glycerol (filled circles). The fluorescence lifetime of BODIPY-C_{10} in the same solvent is shown in blue for comparison.

 This journal is © the Owner Societies 2020

Published on 20 February 2020. Downloaded on 4/30/2020 5:26:52 AM.

Interestingly, the amplitude of the first component also seems to be affected by viscosity – it becomes progressively smaller at higher viscosities and vanishes in the case of the most viscous solvent (70% glycerol–methanol mixture, Fig. S5, ESI†). We hypothesise that this shows that more fluorophores avoid relaxation to $S_{1,m}$ geometry on their path to the ground state at higher viscosities.

Influence of macromolecular crowding

Taking into consideration that biological systems possess many macromolecules whose size is orders of magnitude larger than that of BODIPY-C_{10}, we aimed to investigate how such radical size differences affect its fluorescence lifetime–viscosity dependence. To do so, we used solutions of polymers of varying molecular weight. We note that a polymer molecule, in general, does not remain linear in solution, but instead forms a random coil, which is roughly spherical in shape.[46] The resulting system resembles protein solution and, therefore, could provide us insights into the behaviour of a molecular rotor in a crowded cellular environment. Measurements in actual protein solutions are not possible due to the hydrophobicity of BODIPY-C_{10}. We show that upon the increase in the viscosity of a high weight polymer solution, the lifetimes of BODIPY-C_{10} increase only very slightly compared to measured lifetimes in similar, but micromolecular, systems (Fig. 5A). The lifetimes of BODIPY-C_{10} remain similar to the ones in pure methanol or toluene despite the fact that macroscopic viscosity is increased 1000-fold because of the presence of a polymer.

To explore the effect of macromolecules further, we varied the size of a polymer molecule, PEG in particular, and looked at how this impacts viscosity–lifetime dependence of BODIPY-C_{10}. The average molar masses of PEG polymers were 0.5, 4 and 20 kDa. Their hydrodynamic radii can be estimated from the parameters of Mark–Houwink equation[47] for PEG in methanol, which results in the approximate radii of 0.6, 2 and 4 nm, respectively. By performing a fitting using the lifetime form[3] of the Förster–Hoffmann equation[48] (eqn (3)), we calculated the parameter x, which shows the viscosity sensitivity of a molecular rotor and can have values between 0 and 1.[3]

$$\tau_f = C\eta^x \quad (3)$$

where τ_f is the fluorescence lifetime, C is a constant.

The results demonstrate that parameter x increases 4-fold when the polymer mass is reduced from 20 kDa to 0.5 kDa. Therefore, we find that as the size of the polymer increases, the fluorescence lifetime dependence on the viscosity of the solution decreases (Fig. 5B).

The reason behind the described size dependence is likely to be the following. Molecules, in general, can be affected by surrounding molecules that are not more than ~1 nm distance away.[49,50] Hence, a single molecular rotor is sensitive to a very small volume of the surrounding environment. In a solution of large and heavy polymers, their molar fraction is far smaller compared to the solution of light polymers, even if the mass fractions are the same. As a result, the probability of a large macromolecule finding itself in the volume surrounding a molecular rotor is negligible and the rotor simply exists in a large pocket between polymers (Fig. 5C), which leads to the molecular rotor underestimating bulk viscosity. In the case of a smaller polymers, the probability that such polymers will find themselves next to a molecular rotor is higher, and so the molecular rotor is able to sense the presence of both the solvent and the polymer in its local environment and this leads to a smaller underestimation of viscosity. Such effect of BODIPY-C_{10} sensing only local viscosity, while the bulk viscosity of a system is vastly different, is likely to be true not only for BODIPY-C_{10} but for all molecular rotors in general.

Altogether, polymer solutions illustrate a striking difference between macroscopic viscosity and microviscosity sensed by a molecular rotor. This observation might not be relevant for viscosity studies in lipid membranes, which contain only small

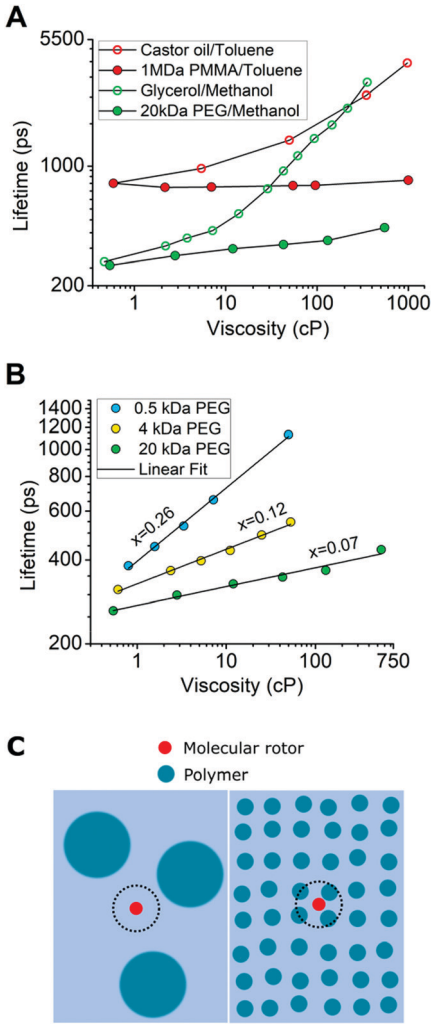

Fig. 5 (A) Fluorescence lifetimes of BODIPY-C_{10} in non-polar Castor oil–toluene and PMMA–toluene solvent mixtures (red dots) and relatively polar glycerol–methanol and PEG–methanol solvent mixtures of varying viscosity (green dots). (B) Linear fit (solid lines) of fluorescence lifetimes (coloured dots) of BODIPY-C_{10} in PEG–methanol polymer solutions of varying viscosity and polymer mass. (C) Scheme depicting the local environment (black dotted circle) of a molecular rotor (red dot) in different weight polymer solutions of the same mass fraction.

Published on 20 February 2020. Downloaded on 4/30/2020 5:26:52 AM.

molecules, but it is crucial for correct quantitative viscosity estimation in other environments with high concentrations of proteins or other macromolecules. Furthermore, if the viscosity obtained by the molecular rotor is then used to assess the diffusion rate of a larger macromolecule, one needs to keep in mind that the macromolecule is likely to experience a higher viscosity than the molecular rotor did.

Conclusions

We have investigated arguably the most applied molecular rotor BODIPY-C_{10} representing widely used family of BODIPY rotors with an ether group, which all have closely similar photophysical properties. We have shown that while this viscosity sensor is insensitive to hydrogen bonding abilities of the environment, it is sensitive to solvent polarity, which has implications in the quantitative determination of viscosity using this rotor. Also, by using femtosecond transient absorption and TD-DFT calculations we have demonstrated that this fluorophore relaxes in a similar manner to other BODIPY rotors. Two processes were observed – partial relaxation to the local minimum of the excited state, which was affected by viscosity but not the polarity of the environment, and complete relaxation from the fluorescent state back to the ground state by overcoming $\sim$0.1 eV energy barrier. This process was affected by both polarity and viscosity and it did not involve any intermediate ''dark'' states. Finally, we have shown that there is a significant discrepancy between microviscosity sensed by BODIPY-C_{10} and the bulk viscosity of solutions of molecules that are significantly larger than the rotor itself. These results implicate that molecular rotors in crowded protein environments are likely to underestimate viscosity and the obtained value will not accurately reflect the viscosity large macromolecules experience in cells. However, this should not be an important factor for microviscosity sensing in lipid membranes, since lipids completely fill the immediate environment of a molecular rotor. Therefore, we expect molecular rotors to provide accurate readings there.

Overall, while BODIPY-C_{10} works well in performing qualitative estimation of viscosity, our results show that accurate quantitative estimation is possible only if two conditions are satisfied. First, BODIPY-C_{10} must be calibrated in solvent mixtures that have the same polarity as the environment in the sample, and second, the surrounding molecules in the sample must not be significantly larger than the rotor itself.

Conflicts of interest

There are no conflicts to declare.

Acknowledgements

This research was funded by a grant (no. S-MIP-19-6) from the Research Council of Lithuania. Quantum chemical computations were carried out using resources at the High-Performance Computing Center ''HPC Sauletekis'' (Vilnius University, Faculty of Physics). We also thank Dr Tatjana Krivorotova and Dr Vaidas Klimkevičius for providing polymers and helping with bulk viscosity measurements.

Notes and references

1 G. S. Zubenko, U. Kopp, T. Seto and L. L. Firestone, *Psychopharmacology*, 1999, **145**, 175–180.
2 O. Nadiv, M. Shinitzky, H. Manu, D. Hecht, C. T. Roberts Jr., D. LeRoith and Y. Zick, *Biochem. J.*, 1994, **298**, 443–450.
3 M. K. Kuimova, *Phys. Chem. Chem. Phys.*, 2012, **14**, 12671–12686.
4 A. Vyšniauskas and M. K. Kuimova, *Int. Rev. Phys. Chem.*, 2018, **37**, 259–285.
5 M. A. Haidekker and E. A. Theodorakis, *Org. Biomol. Chem.*, 2007, **5**, 1669–1678.
6 M. K. Kuimova, G. Yahioglu, J. A. Levitt and K. Suhling, *J. Am. Chem. Soc.*, 2008, **130**, 6672–6673.
7 Y. He, J. Shin, W. Gong, P. Das, J. Qu, Z. Yang, W. Liu, C. Kang, J. Qu and J. S. Kim, *Chem. Commun.*, 2019, **55**, 2453–2456.
8 S.-C. Lee, J. Heo, J.-W. Ryu, C.-L. Lee, S. Kim, J.-S. Tae, B.-O. Rhee, S.-W. Kima and O.-P. Kwon, *Chem. Commun.*, 2016, **52**, 13695–13698.
9 S.-C. Lee, J. Heo, H. C. Woo, J.-A. Lee, Y. H. Seo, C.-L. Lee, S. Kim and O.-P. Kwon, *Chem. – Eur. J.*, 2018, **24**, 13706–13718.
10 J. A. Levitt, P.-H. Chung, M. K. Kuimova, G. Yahioglu, Y. Wang, J. Qu and K. Suhling, *ChemPhysChem*, 2011, **12**, 662–672.
11 M. Köllner and J. Wolfrum, *Chem. Phys. Lett.*, 1992, **200**, 199–204.
12 N. A. Hosny, C. Fitzgerald, C. Tong, M. Kalberer, M. K. Kuimova and F. D. Pope, *Faraday Discuss.*, 2013, **165**, 343–356.
13 J. M. Nölle, C. Jüngst, A. Zumbusch and D. Wöll, *Polym. Chem.*, 2014, **5**, 2700–2703.
14 N. A. Hosny, G. Mohamedi, P. Rademeyer, J. Owen, Y. Wu, M.-X. Tang, R. J. Eckersley, E. Stride and M. K. Kuimova, *Proc. Natl. Acad. Sci. U. S. A.*, 2013, **110**, 9225–9230.
15 Y. Wu, M. Štefl, A. Olzyńska, M. Hof, G. Yahioglu, P. Yip, D. R. Casey, O. Ces, J. Humpolíčková and M. K. Kuimova, *Phys. Chem. Chem. Phys.*, 2013, **15**, 14986–14993.
16 M. R. Dent, I. López-Duarte, C. J. Dickson, N. D. Geoghegan, J. M. Cooper, I. R. Gould, R. Krams, J. A. Bull, N. J. Brooks and M. K. Kuimova, *Phys. Chem. Chem. Phys.*, 2015, **17**, 18393–18402.
17 M. Olšinová, P. Jurkiewicz, M. Pozník, R. Šachl, T. Prausová, M. Hof, V. Kozmík, F. Teplý, J. Svobodab and M. Cebecauer, *Phys. Chem. Chem. Phys.*, 2014, **16**, 10688–10697.
18 A. Vyšniauskas, M. Qurashi and M. K. Kuimova, *Chem. – Eur. J.*, 2016, **22**, 13210–13217.
19 P. S. Sherin, I. López-Duarte, M. R. Dent, M. Kubánková, A. Vyšniauskas, J. A. Bull, E. S. Reshetnikova, A. S. Klymchenko, Y. P. Tsentalovich and M. K. Kuimova, *Chem. Sci.*, 2017, **8**, 3523–3528.
20 L. E. Shimolina, M. A. Izquierdo, I. López-Duarte, J. A. Bull, M. V. Shirmanova, L. G. Klapshina, E. V. Zagaynova and M. K. Kuimova, *Sci. Rep.*, 2017, **7**, 41097.

 This journal is © the Owner Societies 2020

Published on 20 February 2020. Downloaded on 4/30/2020 5:26:52 AM.

21 I. López-Duarte, T. T. Vu, M. A. Izquierdo, J. A. Bulla and M. K. Kuimova, *Chem. Commun.*, 2014, **50**, 5282–5284.
22 M. Kubánková, I. López-Duarte, D. Kiryushko and M. K. Kuimova, *Soft Matter*, 2018, **14**, 9466–9474.
23 M. Kubánková, P. A. Summers, I. López-Duarte, D. Kiryushko and M. K. Kuimova, *ACS Appl. Mater. Interfaces*, 2019, **11**, 36307–36315.
24 Z. Yang, Y. He, J. H. Lee, W.-S. Chae, W. X. Ren, J. H. Lee, C. Kang and J. S. Kim, *Chem. Commun.*, 2014, **50**, 11672–11675.
25 G. Ferri, L. Nucara, T. Biver, A. Battisti, G. Signore and R. Bizzarri, *Biophys. Chem.*, 2016, **208**, 17–25.
26 I. E. Steinmark, A. L. James, P.-H. Chung, P. E. Morton, M. Parsons, C. A. Dreiss, C. D. Lorenz, G. Yahioglu and K. Suhling, *PLoS One*, 2019, **14**, e0211165.
27 C. Wang, X. Song, L. Chen and Y. Xiao, *Biosens. Bioelectron.*, 2017, **91**, 313–320.
28 J. E. Chambers, M. Kubánková, R. G. Huber, I. López-Duarte, E. Avezov, P. J. Bond, S. J. Marciniak and M. K. Kuimova, *ACS Nano*, 2018, **12**, 4398–4407.
29 A. Vyšniauskas, I. López-Duarte, N. Duchemin, T.-T. Vu, Y. Wu, E. M. Budynina, Y. A. Volkova, E. P. Cabrera, D. E. Ramírez-Ornelasc and M. K. Kuimova, *Phys. Chem. Chem. Phys.*, 2017, **19**, 25252–25259.
30 J. A. Levitt, M. K. Kuimova, G. Yahioglu, P.-H. Chung, K. Suhling and D. Phillips, *J. Phys. Chem. C*, 2009, **113**, 11634–11642.
31 J. Speight, *Lange's Handbook of Chemistry*, McGraw-Hill Professional, New York, 2016.
32 M. J. Frisch, *et al.*, *Gaussian09, Revision D.01*, Gaussian, Inc., Wallingford CT, 2013.
33 R. G. Parr and W. Yang, *Density-Functional Theory of Atoms and Molecules*, Oxford University Press, Oxford, 1989.
34 R. E. Stratmann, G. E. Scuseria and M. J. Frisch, *J. Chem. Phys.*, 1998, **109**, 8218–8224.
35 Y. Zhao and D. G. Truhlar, *Theor. Chem. Acc.*, 2008, **120**, 215–241.
36 R. A. Kendall, T. H. Dunning and R. J. Harrison, *J. Chem. Phys.*, 1992, **96**, 6796–6806.
37 M. Cossi, N. Rega, G. Scalmani and V. Barone, *J. Comput. Chem.*, 2003, **24**, 669–681.
38 J. R. Lakowicz, *Principles of Fluorescence Spectroscopy*, Springer Science & Business Media, 2006.
39 J. J. Snellenburg, S. Laptenok, R. Seger, K. M. Mullen and I. H. M. van Stokkum, *J. Stat. Softw.*, 2012, **49**, 1–22.
40 T. Suhina, S. Amirjalayer, S. Woutersen, D. Bonn and A. M. Brouwer, *Phys. Chem. Chem. Phys.*, 2017, **19**, 19998–20007.
41 S. Toliautas, J. Dodonova, A. Žvirblis, I. Čiplys, A. Polita, A. Devižis, S. Tumkevičius, J. Šulskus and A. Vyšniauskas, *Chem. – Eur. J.*, 2019, **25**, 10342–10349.
42 A. Prlj, L. Vannay and C. Corminboeuf, *Helv. Chim. Acta*, 2017, **100**, e1700093.
43 A. Prlj, A. Fabrizio and C. Corminboeuf, *Phys. Chem. Chem. Phys.*, 2016, **18**, 32668–32672.
44 F. Li, S. I. Yang, Y. Ciringh, J. Seth, C. H. Martin, D. L. Singh, D. Kim, R. R. Birge, D. F. Bocian, D. Holten and J. S. Lindsey, *J. Am. Chem. Soc.*, 1998, **120**, 10001–10017.
45 H. L. Kee, C. Kirmaier, L. Yu, P. Thamyongkit, W. J. Youngblood, M. E. Calder, L. Ramos, B. C. Noll, D. F. Bocian, W. R. Scheidt, R. R. Birge, J. S. Lindsey and D. Holten, *J. Phys. Chem. B*, 2005, **109**, 20433–20443.
46 I. Teraoka, *Polymer Solutions: An Introduction to Physical Properties*, John Wiley & Sons, New York, 2002.
47 M. P. J. Dohmen, A. M. Pereira, J. M. K. Timmer, N. E. Benes and J. T. F. Keurentjes, *J. Chem. Eng. Data*, 2008, **53**, 63–65.
48 T. Förster and G. Hoffmann, *Z. Phys. Chem.*, 1971, **75**, 63–76.
49 Z. Zhang, S. Ryu, Y. Ahn and J. Jang, *Phys. Chem. Chem. Phys.*, 2018, **20**, 30492–30501.
50 A. Choudhary and A. Chandra, *Phys. Chem. Chem. Phys.*, 2016, **18**, 6132–6145.